

RESEARCH

Open Access



Resources recovery-rubidium recovery from desalination brine through hydrometallurgy techniques

Cheng-Han Lee^{1,2}, Wei-Sheng Chen^{1,2*} and Fan-Wei Liu³

Abstract

Because of the water scarcity in many regions, different methods have been implemented to address this problem. The desalination technique is known as a practical solution among them. However, brine from the desalination process, which contains high concentrations of salts, minerals, and chemicals, will cause environmental harm to the sea, soil, and groundwater if it is not properly treated. Therefore, recovering critical resources from brine is essential for reducing brine disposal. This study aims to apply two hydrometallurgy systems, namely ion exchange and ionic liquid extraction, to circulate rubidium resources from brine. Dowex G26 resin was employed in the ion exchange system, and the adsorption isotherm model and saturated adsorption capacity were explored initially. The optimal parameters such as pH value, L/S ratio (liquid/solid), adsorption period, and adsorption temperature will then be investigated. In the ionic liquid extraction process, the t-BAMBP/C₂mimNTf₂ system (4-tert-Butyl-2-(α -methylbenzyl)phenol/1-ethyl-3-methylimidazolium bis(trifluoromethylsulfonyl)imide) was used, and the parameters including pH value, concentrations of t-BAMBP, (O+I)/A ratio (organic + ionic liquid/aqueous), extraction time, and extraction temperature will be optimized as well. The results reveal that adsorption capacity and extraction efficiencies were 14.3 mg g⁻¹ and 86%, respectively. Furthermore, suitable reagents, including HCl and HNO₃, were applied to desorb and strip rubidium from the Dowex G26 and t-BAMBP/C₂mimNTf₂ systems. To sum up, environmental hazards of desalination brine and rubidium resources can be reduced and recovered through the two different extraction systems.

Keywords Rubidium, Desalination brine, Ion exchange, Ionic liquid extraction, Dowex G26, C₂mimNTf₂, Resource circulation

*Correspondence:

Wei-Sheng Chen
kenchen@mail.ncku.edu.tw

¹Department of Resources Engineering, National Cheng Kung University,
701401 Tainan, Taiwan

²Hierarchical Green-Energy Materials (Hi-GEM) Research Center, National
Cheng Kung University, 701401 Tainan, Taiwan

³Academy of Circular Economy, National Chung Hsing University,
540216 Nantou County, Taiwan



© The Author(s) 2024. **Open Access** This article is licensed under a Creative Commons Attribution 4.0 International License, which permits use, sharing, adaptation, distribution and reproduction in any medium or format, as long as you give appropriate credit to the original author(s) and the source, provide a link to the Creative Commons licence, and indicate if changes were made. The images or other third party material in this article are included in the article's Creative Commons licence, unless indicated otherwise in a credit line to the material. If material is not included in the article's Creative Commons licence and your intended use is not permitted by statutory regulation or exceeds the permitted use, you will need to obtain permission directly from the copyright holder. To view a copy of this licence, visit <http://creativecommons.org/licenses/by/4.0/>.

1 Introduction

Water scarcity has become a more pressing issue in many regions due to various factors. These include a growing population, higher per capita water consumption, and economic development, all leading to increased demand for water. At the same time, climate change and water contamination are reducing the availability of water resources, further exacerbating the problem [1]. According to the statistics, roughly 30% of the world's population will face water scarcity by 2025 [2]. As a result, there is a growing urgency to develop cost-effective and efficient technologies for producing and supplying freshwater now [3]. Among various methods, the desalination process is known as a practical solution to address this global problem. Desalination is a procedure which involves removing salt and other minerals from seawater, brackish water, or other types of water which are not suitable for human consumption or industrial use [4]. Nowadays, there are several techniques for desalination, including distillation, reverse osmosis, and electro dialysis processes [5]. By improving these techniques, desalination has become an increasingly important solution for water-scarce areas, providing a reliable source of freshwater for drinking, irrigation, and industrial applications [6]. Although desalination can provide freshwater and reduce water usage from nature (glacier water and groundwater), energy consumption is high, and the disposal of brine, a byproduct of the process, is also a critical problem [7–9].

Desalination brine contains high concentrations of salts, minerals, and chemicals, all from seawater or the desalination process [10]. There are roughly 20,000 desalination plants worldwide, and the volume of daily disposal brine now reaches about 142 million m³ [11, 12]. Because brine is a concentrated stream, brine disposal will cause environmental harm, such as eutrophication, proliferation of harmful algae, decreasing dissolved oxygen, and pH fluctuation of seawater. For brine management, direct disposal, brine minimization, and direct reuse are considered. Direct disposal method, including surface discharge, sewer discharge, evaporation ponds, land application, and deep well injection, are commonly used now [13, 14]. Nevertheless, all disposal methods have varying levels of adverse environmental effects, like marine pollution, groundwater pollution, and soil salinization [15]. For instance, surface discharge would pollute marine ecosystems by increasing salinity and pH value. Deep well injection would contaminate groundwater and nearby water aquifers [16]. Therefore, brine minimization and direct reuse have gradually gained attention. Although brine minimization can reduce the amount of brine, the energy consumption is high, and the brine problem is not resolved thoroughly [17]. In the direct reuse method, carbon capture and resources recovery are the major applications of brine [18]. Abundant sodium,

potassium, magnesium, and calcium in brine can react with CO₂ through the Solvay Process/Modified Solvay Process and amine carrier method to produce useful carbonate products [19–24]. In addition to sodium, potassium, magnesium, and calcium, there are also many critical metals in brine (Table S1) [11]. These metals originally came from ore exploitation, such as sodalite, orthoclase, calcite, ulexite, and so on, which would easily cause environmental hazards during the mining processes. Hence, it can reduce the side effects and enhance the brine's value if these metals can be recovered and extracted from the brine.

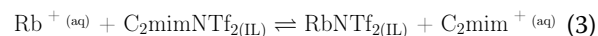
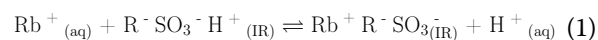
The objective of this study was then to recover rubidium resources from brine through hydrometallurgical techniques. Rubidium is a versatile element utilized in various industries. It can be used in television, radar systems, infrared filters, radiant energy receivers, and reconnaissance telescopes. Additionally, rubidium carbonate is an essential raw material for glass production, enhancing stability and durability. Rubidium chloride, for instance, is employed in manufacturing sleeping pills, sedatives, and treatments for bipolar disorder. Hydrometallurgy is a branch of metallurgy which extracts, separates, and purifies metals from solutions [25]. Common separation and purification methods of hydrometallurgy include chemical precipitation, solvent extraction, ion exchange, and ionic liquid extraction [26] with ion exchange and ionic liquid extraction applied in this study. Ion exchange is a procedure in which ions are exchanged between a solid and a liquid, typically applying an exchange resin to conduct the procedure [27]. The exchange resin would contain functional groups which attract and exchange ions of the same or similar charges. Ion exchange is employed for various applications, such as water softening, purification, and separation, as well as in producing food, beverages, and pharmaceuticals [28]. On the other hand, ionic liquid extraction is a separation process which uses ionic liquids to extract metals. The ionic liquid is a kind of salt which exists in a liquid state at room temperature (melting point below 100 °C), and its advantages over traditional organic extractants are high thermal stability, low volatility, and tunable properties [29]. Moreover, it can not only be an extractant to extract metals but also be a diluent to enhance the extraction ability with other conventional extractants [30]. Currently, ion exchange and ionic liquid methods are used to recover metals from waste. For example, gold and silver can be recovered from waste-printed circuit boards using MTA 5011 resin [31], and copper, lead, and nickel can be circulated from semiconductor wastes through Chelex-100 [32]. Besides, imidazolium and phosphonium ionic liquids are majorly applied for resources circulation from waste electronic products, solutions, and NdFeB magnets [33–39].

The ion exchange resin and ionic liquid used in this study for rubidium circulation were Dowex G26 resin and $C_2mimNTf_2$ (1-ethyl-3-methylimidazolium bis(trifluoromethylsulfonyl)imide). Both have already exhibited excellent separation ability in numerous studies [40–45]. The experiments of the two systems will be separately conducted, and the results will be compared to show their merits and drawbacks. In the Dowex G26 system, the adsorption isotherms, described by means of the Freundlich and Langmuir isotherms, were employed to explore the adsorption behaviors of rubidium through the Dowex G26 system first. Subsequently, the optimal parameters of rubidium adsorption, such as pH value, L/S ratio (liquid-solid ratio), and adsorption period, were investigated. Moreover, the thermodynamic parameters, such as enthalpy, entropy, and Gibbs free energy, will also be shown. Finally, the most suitable desorption reagent, the concentration of the desorption reagent, and the desorption L/S ratio will be revealed to obtain rubidium compounds. In the $C_2mimNTf_2$ system, $C_2mimNTf_2$ was a diluent to collocate with t-BAMBP (4-tert-Butyl-2-(α -methylbenzyl), which both are common for rubidium extraction [43, 46]. The optimal conditions of rubidium recovery through the t-BAMBP/ $C_2mimNTf_2$ system will also be investigated in this research. In summary, this study aims to address the problem of brine disposal and enhance its value. Simultaneously, rubidium resources could be acquired to reach the goal of wastewater treatment/management and resources recovery.

2 Materials and methods

2.1 Reagents and chemicals

The desalination brine in this study was from the desalination plant in Taiwan, and the concentrations of the major elements after pretreatment, including pH swing method, filtration, and concentration, are shown in Table 1. Dowex G26 in the ion exchange experiment was purchased from Lenntech (Delfgauw, Netherlands) and applied to adsorb rubidium from desalination brine. It is a strong acid exchange resin which can adsorb cation ions by releasing H^+ (Eq. (1)) [41]. Its basic information is shown in Table S2. t-BAMBP ($\geq 90\%$) was bought from Realkan Corporation (Beijing, China) as the extractant for the extraction process, and $C_2mimNTf_2$ ($\geq 97\%$) as a diluent was obtained from Sigma-Aldrich (St. Louis, USA). Their chemical structures and extraction mechanisms are displayed in Fig. S1 and Eqs. (2) and (3) [44, 46]. The information on other reagents and chemicals is illustrated in Supplementary Materials (Reagents and chemicals-other reagents and chemicals).



2.2 Apparatuses

The major apparatuses of this research were inductively coupled plasma optical emission spectrometry (ICP-OES, Avio 220 Max ICP-OES, PerkinElmer, Waltham, MA, USA) and pH meter (6177 M, Jenco Instruments, Taipei City, Taiwan). Their information and introduction of other apparatuses are shown in Supplementary Materials (Apparatuses-information and other apparatuses).

2.3 Ion exchange and ionic extraction process

In this research, Dowex G26 was initially contacted with different concentrations of rubidium carbonate solutions to explore the adsorption isotherm model and its saturated adsorption capacity. Afterward, Dowex G26 was contacted with desalination brine to adsorb rubidium ions. As soon as the adsorption process was finished, HNO_3 , HCl , H_2SO_4 , and NH_4OH were employed in the desorption procedure to find the most suitable desorption reagent.

In the ionic liquid extraction part, t-BAMBP was diluted into $C_2mimNTf_2$ to extract rubidium from brine. The parameters such as pH value, t-BAMBP concentration, (O+I)/A ratio (organic+ionic liquid/aqueous ratio), extraction time, and extraction temperature will be investigated. After the extraction process, HNO_3 , HCl , H_2SO_4 , and NH_4OH were applied to strip rubidium from the organic phase to the aqueous phase. The most suitable stripping reagent will be decided, and the parameters involved concentration of the stripping reagent, (O+I)/A ratio, and stripping time were then investigated. The complete information and processes of the two systems are revealed in Supplementary Materials (Ion exchange and ionic extraction process-complete information).

3 Results and discussion

3.1 Ion exchange procedure

3.1.1 Adsorption isotherm model and adsorption capacity of Dowex G26 resin

Dowex G26 was contacted with different initial concentrations (10 to 1200 $mg L^{-1}$) of rubidium carbonate solutions under an L/S ratio of 1000 for 1024 min at 298 K to determine the adsorption isotherm models. Figure 1 shows the relationship between C_e and q_e , and

Table 1 The concentrations of the major elements in desalination brine after pretreatment

Elements	Na	K	Rb	Ca	Mg	Li
Concentration ($mg L^{-1}$)	19,710	734	48	43	41	20

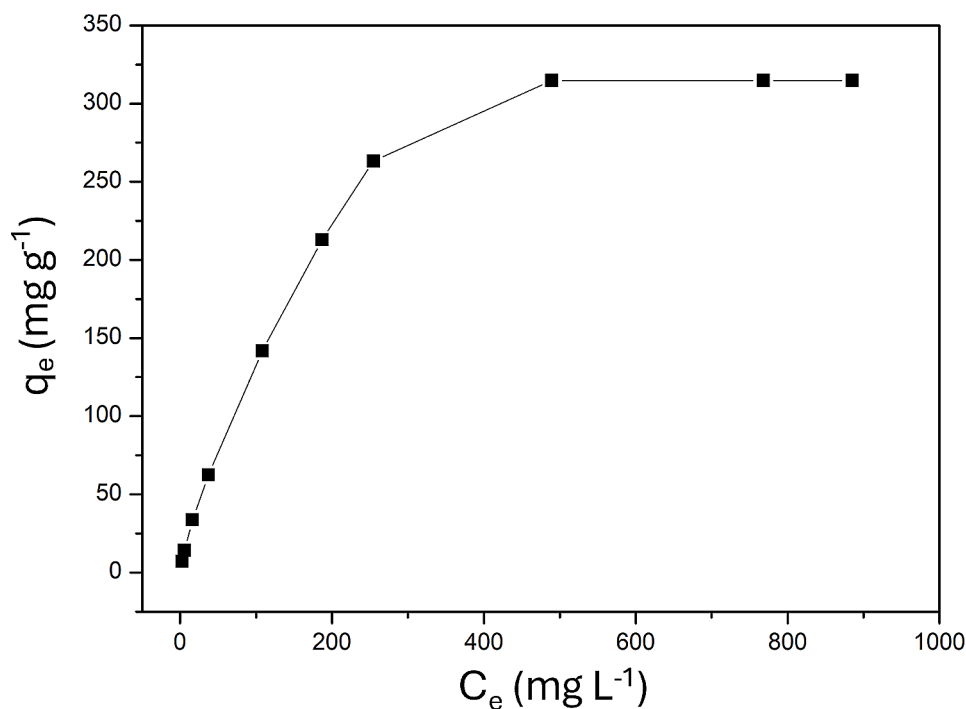


Fig. 1 The relationship between C_e and q_e of rubidium adsorption through Dowex G26

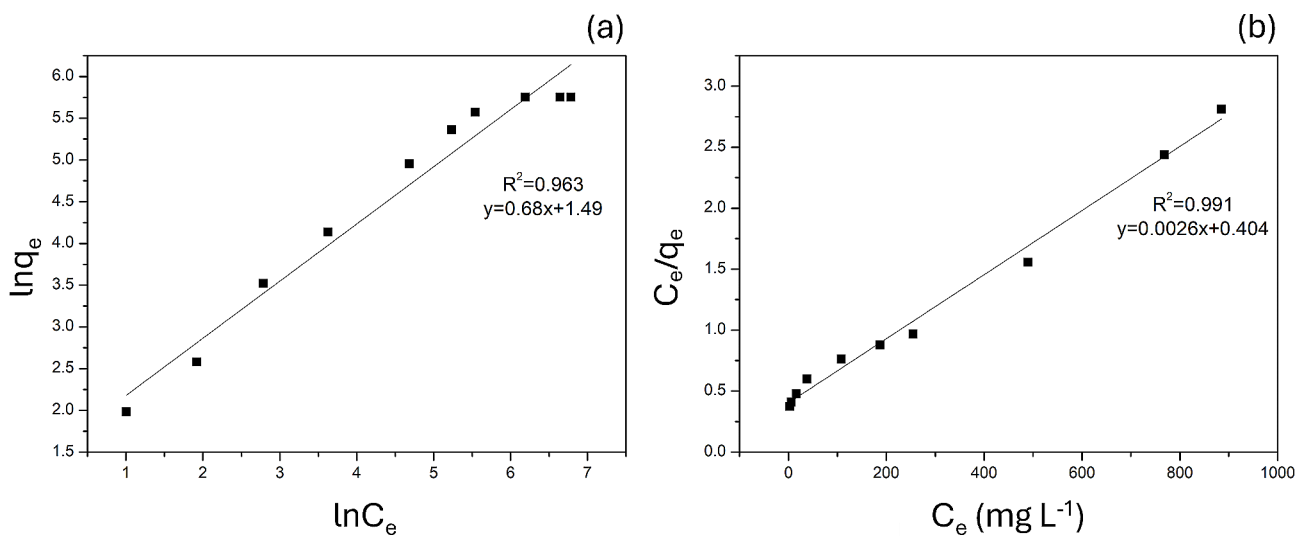


Fig. 2 The adsorption capacity of rubidium through Dowex G26 (a) Freundlich Model (b) Langmuir Model

the saturated adsorption capacity of rubidium through Dowex G26 was approximately 315 mg g^{-1} based on the figure. Freundlich and Langmuir models could then be generated through Fig. 1, Eqs. (S1) and (S2) [47–48]. The calculation processes and values of n , K_F , q_m , and K_L are shown in Table S3. Furthermore, Fig. 2a and b illustrate that the R^2 in the Freundlich and Langmuir models were individually 0.963 and 0.991. A higher R^2 of the Langmuir model illustrates that the rubidium adsorption through Dowex G26 conforms to the Langmuir model, and the precise saturated adsorption capacity was 385 mg g^{-1} . In

addition, it represents that rubidium adsorption occurred at specific binding sites which were localized on the surface of the Dowex G26, and each site can hold at most one molecule of rubidium.

In the previous research, the saturated adsorption capacity of cesium through Dowex G26 was 456 mg g^{-1} , and the adsorption behavior also fit with the Langmuir model [49]. The difference between the two elements is that the hydrated ionic radius of cesium is smaller than rubidium. Under the same valence, the affinity of Dowex

G26 for cesium is higher than that of rubidium due to its small hydrated ionic radius.

3.1.2 Adsorption pH value

Although many metal ions existed in the desalination brine, only rubidium, potassium, and sodium could be efficiently adsorbed through Dowex G26 due to its high selectivity. Thus, the following discussion only focuses on their adsorption capacities.

The adsorption pH value was initially examined in this research and was adjusted from pH 9 to 14 (the original pH value of brine after pretreatment was 8.5). Other fixed parameters were an L/S ratio of 1000, adsorption period for 1024 min, and adsorption temperature at 298 K. Figure 3a reveals that the adsorption capacities increased when the initial pH value was enhanced. The reason is that Dowex G26 is a strong acid exchange resin, so it can release more H^+ at higher initial pH values. Besides, it

was found that despite Dowex G26 having a higher selectivity for rubidium and potassium compared to sodium ($Rb > K >> Na$), the sodium adsorption capacity was the highest among the three metals. This is likely due to the significantly higher concentrations of sodium and potassium than rubidium in the brine, resulting in more significant adsorption through Dowex G26. To avoid interference from other metals and minimize chemical usage, pH 9 was selected for the initial pH value.

3.1.3 Adsorption L/S ratio

L/S ratios ranging from 100 to 2000 were tested, while the pH was kept at 9, the adsorption period was 1024 min, and the adsorption temperature was 298 K. As shown in Fig. 3b, the adsorption capacities increased with decreasing L/S ratio. For example, the adsorption capacity of rubidium increased from 5.5 to 39 $mg\ g^{-1}$ as the ratio decreased from 2000 to 100. This phenomenon indicates

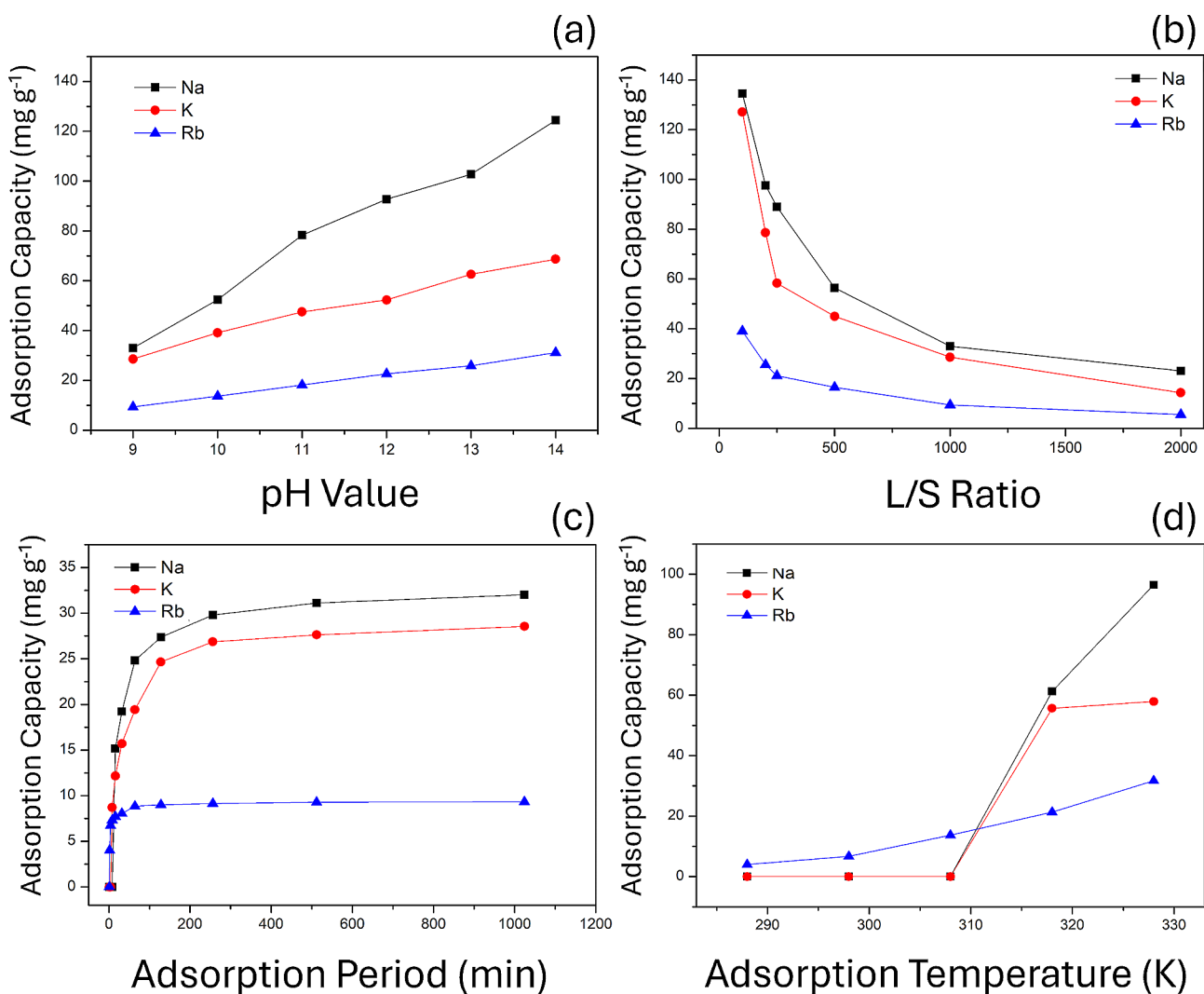


Fig. 3 Adsorption capacities of Na, K, and Rb at different (a) pH values (b) L/S ratios (c) adsorption periods (d) adsorption temperatures

that enough Dowex G26 could adsorb more metal ions from the brine. Nonetheless, high amounts of impurities such as Na and K were adsorbed through excessive Dowex G26 because they have much higher initial concentrations than Rb. Thus, an L/S ratio of 1000 was chosen to minimize the amount of Dowex G26 used, reduce impurity levels, and get as much rubidium as possible.

3.1.4 Adsorption period

Adsorption periods were regulated from 1 min to 1024 min, with fixed parameters of pH 9, L/S ratio of 1000, and adsorption temperature at 298 K. Figure 3c displays that the adsorption period was a crucial parameter in the ion exchange process. Only rubidium was found to be adsorbed through Dowex G26 in 4 min, and the reaction reached equilibrium after 64 min. On the other hand, potassium and sodium were adsorbed through Dowex G26 at 8 and 16 min, respectively, and took longer than rubidium to reach equilibrium –128 min for potassium and 512 min for sodium. This suggests that the affinity between Dowex G26 and the metals affects the reaction rate, and the adsorption period for 4 min was chosen for this study. Under this condition, only rubidium was adsorbed, with an adsorption capacity of 6.7 mg g⁻¹.

3.1.5 Adsorption temperature and thermodynamics

To obtain more rubidium resources, adsorption temperatures were tested from 288 to 328 K, while other fixed parameters were pH 9, L/S ratio of 1000, and adsorption period for 4 min. Figure 3d demonstrates that the adsorption capacity of rubidium increased from 3.6 to 31 mg g⁻¹ as the temperatures rose from 288 to 328 K. Moreover, potassium and sodium were also adsorbed through Dowex G26 at 318 and 328 K, even if the adsorption period was only 4 min. These observations suggest that

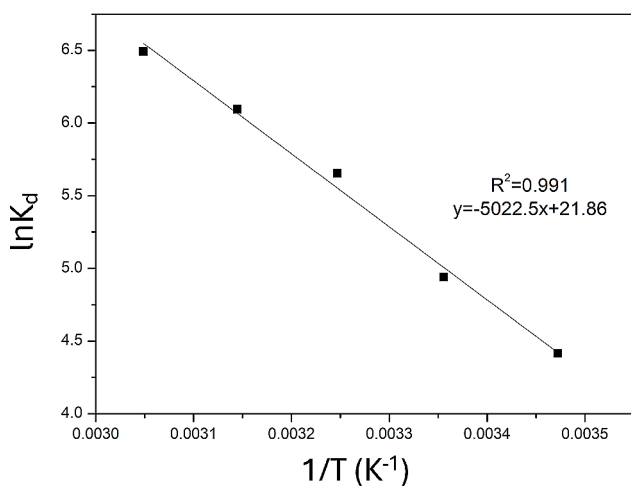


Fig. 4 Relationship of partition coefficient in natural logarithm scale with 1/T

the adsorption behavior of Dowex G26 may be an endothermic reaction, and an appropriate increase in temperature is advantageous to the reaction. Based on the results, adsorption temperature at 308 K was chosen to avoid the adsorption of potassium and sodium, and the adsorption capacity of rubidium was 14 mg g⁻¹.

To determine the thermodynamics data of rubidium adsorption, the relationship between the partition coefficient of rubidium adsorption in natural logarithm scale and 1/T was acquired from Fig. 3d (see Fig. 4). Enthalpy, entropy, and Gibbs free energy were subsequently calculated through Eqs. (S3) to (S7). Table S4 reveals that ΔG_s were negative at all temperatures, manifesting that the rubidium adsorption through Dowex G26 is a spontaneous reaction. Additionally, ΔS and ΔH are positive, indicating that the adsorption behavior is favorable at high temperatures, a characteristic which is consistent with most commercial resins.

3.1.6 Desorption procedure

After adsorption through Dowex G26, 14 mg g⁻¹ of rubidium was in the resin, and different reagents such as HNO₃, HCl, H₂SO₄, and NH₄OH were applied to desorb rubidium from the resin to the aqueous phase. The fixed parameters were 1 M, L/S ratio 1000, desorption period for 256 min, and desorption temperature at 298 K. According to Fig. 5, it can be noticed that the acid solutions were effective in desorbing rubidium from Dowex G26. Because Dowex G26 resin is a strong acid exchange resin, it requires much H⁺ to exchange with rubidium ions. Therefore, HCl, with the highest desorption efficiency (94%) among the three acids, was selected as the desorption reagent in this study.

Once the suitable reagent was decided, its concentration, desorption L/S ratio, and desorption period were explored. Figure 6a and c display the optimal parameters were 2 M, L/S ratio 200, and desorption period for 64 min. Under these situations, the desorption efficiency was 93%. It can be discovered that the optimal L/S ratio was not high when the concentration of HCl was adequate during the desorption process, and the concentration of rubidium could be enriched due to less volume of HCl. Nevertheless, the desorption period was longer than the adsorption period, demonstrating that the desorption process required more time to exchange Rb⁺ with H⁺. After the desorption process, the concentrations of metals are in Table 2.

3.2 Ionic liquid extraction process

Although there were many elements in desalination brine, only rubidium and potassium could be efficiently extracted through t-BAMBP/C₂mimNTf₂ due to the selectivity of t-BAMBP/C₂mimNTf₂ are Cs>Rb>>K >>

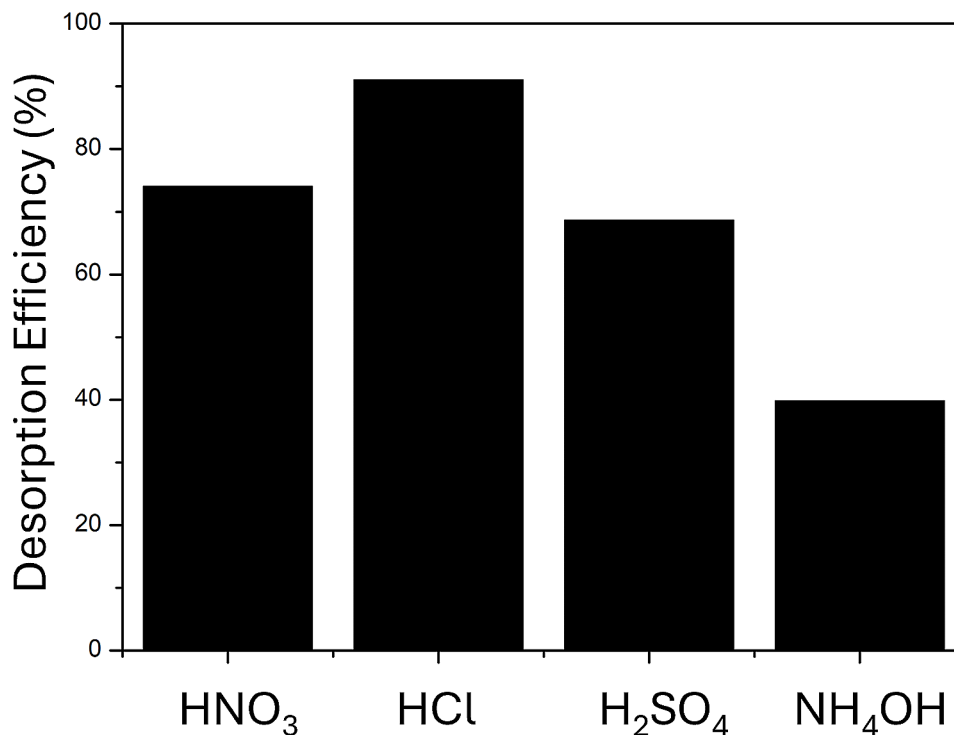


Fig. 5 Desorption efficiency of rubidium through different reagents (desorption period for 256 min)

Na >> Li. Thus, only two elements' extraction efficiencies are demonstrated in this part.

3.2.1 Extraction pH value

pH values were varied from 9 to 14 in the t-BAMBP/ $C_2mimNTf_2$ system, whereas fixed parameters were 1 M t-BAMBP, (O+I)/A ratio 1, extraction time for 15 min, and extraction temperature at 298 K. Figure 7a reveals that the extraction of potassium and rubidium through the t-BAMBP/ $C_2mimNTf_2$ system was efficient with increasing pH values. The reason is that both t-BAMBP and $C_2mimNTf_2$ have a higher affinity for metal ions under alkaline conditions [43, 50]. Nonetheless, it can be found that the extraction efficiencies of the two metals declined at pH 13 and 14. This is because the emulsification occurred in the t-BAMBP/ $C_2mimNTf_2$ system under strong alkaline conditions, which can block the contact between the two phases and reduce extraction efficiency. Therefore, pH 9 was optimal for this process, which reduced the usage of chemicals and the extraction amount of potassium.

3.2.2 t-BAMBP concentration

t-BAMBP concentrations were regulated from 0.1 to 2 M in this process, and other fixed parameters were pH 9, (O+I)/A ratio 1, extraction time for 15 min, and extraction temperature at 298 K. Figure 7b demonstrates that the rubidium extraction through the t-BAMBP/ $C_2mimNTf_2$ system enhanced when t-BAMBP

concentration was from 0.1 to 0.5 M and reach stable at 0.5 M of t-BAMBP. An excessive amount of t-BAMBP would make the extraction efficiency of potassium gradually increase, resulting in a decrease in rubidium's purity from 23 to 17%. Therefore, 0.5 M of t-BAMBP was decided, and the extraction efficiencies of rubidium and potassium were 84 and 18%, respectively.

3.2.3 (O+I)/A ratio

(O+I)/A ratios were adjusted between 0.1 and 2, while the fixed parameters were pH 9, 0.5 M t-BAMBP, extraction time for 15 min, and extraction temperature at 298 K. Figure 7c shows that the extraction efficiency of rubidium did not change much (<5%) when the (O+I)/A ratio increased, suggesting that the influence of the (O+I)/A ratio on the extraction efficiency of rubidium was small. In contrast, the extraction efficiency of potassium was mounting above 20% as the (O+I)/A ratio enhanced. This phenomenon indicates that t-BAMBP and $C_2mimNTf_2$ would preferentially extract rubidium. As a result, an excessive $C_2mimNTf_2$ would start to extract potassium, leading to a large extraction amount of potassium. Based on these findings, (O+I)/A ratio of 0.1 was chosen, and the concentration could be enriched due to the lower volume of extractant and diluent.

3.2.4 Extraction time

Extraction time was set up from 1 to 60 min in this process, and the fixed parameters were kept at pH 9, 0.5 M

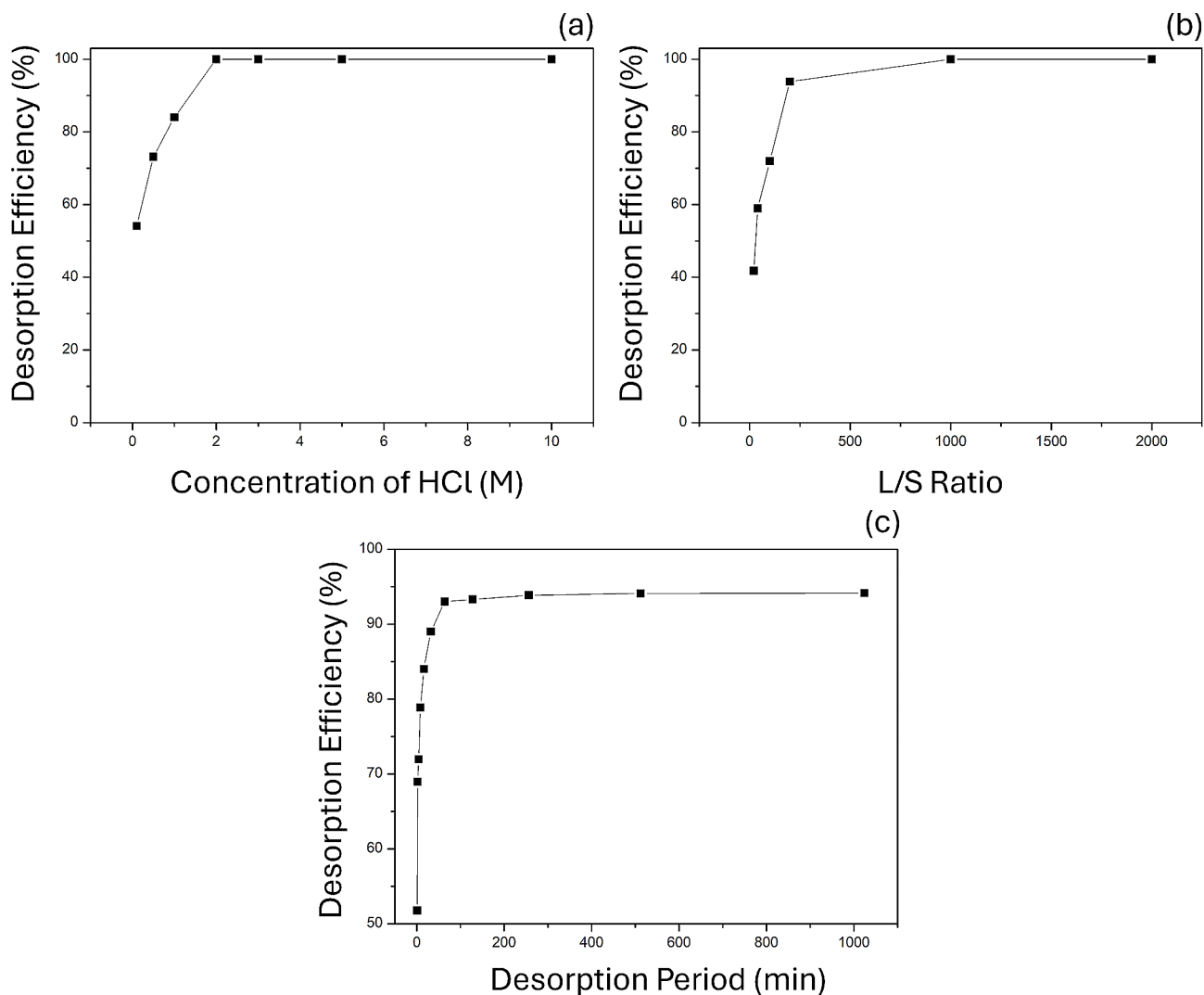


Fig. 6 Rubidium desorption through HCl (a) concentration of HCl (b) L/S ratio (c) desorption period

Table 2 Metal concentrations after ion exchange process (Recovery efficiency of rubidium: 28%)

Elements	Rb	Na	K	Mg	Ca	Li
Concentration (mg L ⁻¹)	66.5	0.9	0.4	N.D.	N.D.	N.D.

t-BAMBP, (O+I)/A ratio of 0.1, and extraction temperature at 298 K. Figure 7d illustrates that the extraction behaviour through the t-BAMBP/C₂mimNTf₂ system was relatively slow. Both the potassium and rubidium extraction reactions reached equilibrium after 30 min of extraction. The possible reason is that the viscosity of C₂mimNTf₂ is higher than typical diluents, contributing to the slower extraction rate, as the system required more time to mix thoroughly (The viscosities of C₂mimNTf₂ and typical diluents are demonstrated in Table S5 [49]). Therefore, a 30 min extraction time was chosen in this research to ensure a complete reaction and obtain more rubidium resources.

3.2.5 Extraction temperature and thermodynamics

In this part, extraction temperatures ranged from 288 to 328 K, and fixed parameters were pH 9, 0.5 M t-BAMBP, (O+I)/A ratio of 0.1, and extraction time for 30 min. Figure 7e reveals that the extraction efficiencies of potassium and rubidium decreased as the reaction temperature increased. The reason is that the extraction of metals through t-BAMBP is an exothermic reaction, so a lower temperature is more favorable for this procedure [51]. However, the decline in extraction efficiency with increasing temperature was not as significant as t-BAMBP dissolved in common diluents [50, 51]. This is because C₂mimNTf₂, the ionic liquid used in this experiment, also has extraction ability, enabling the extraction

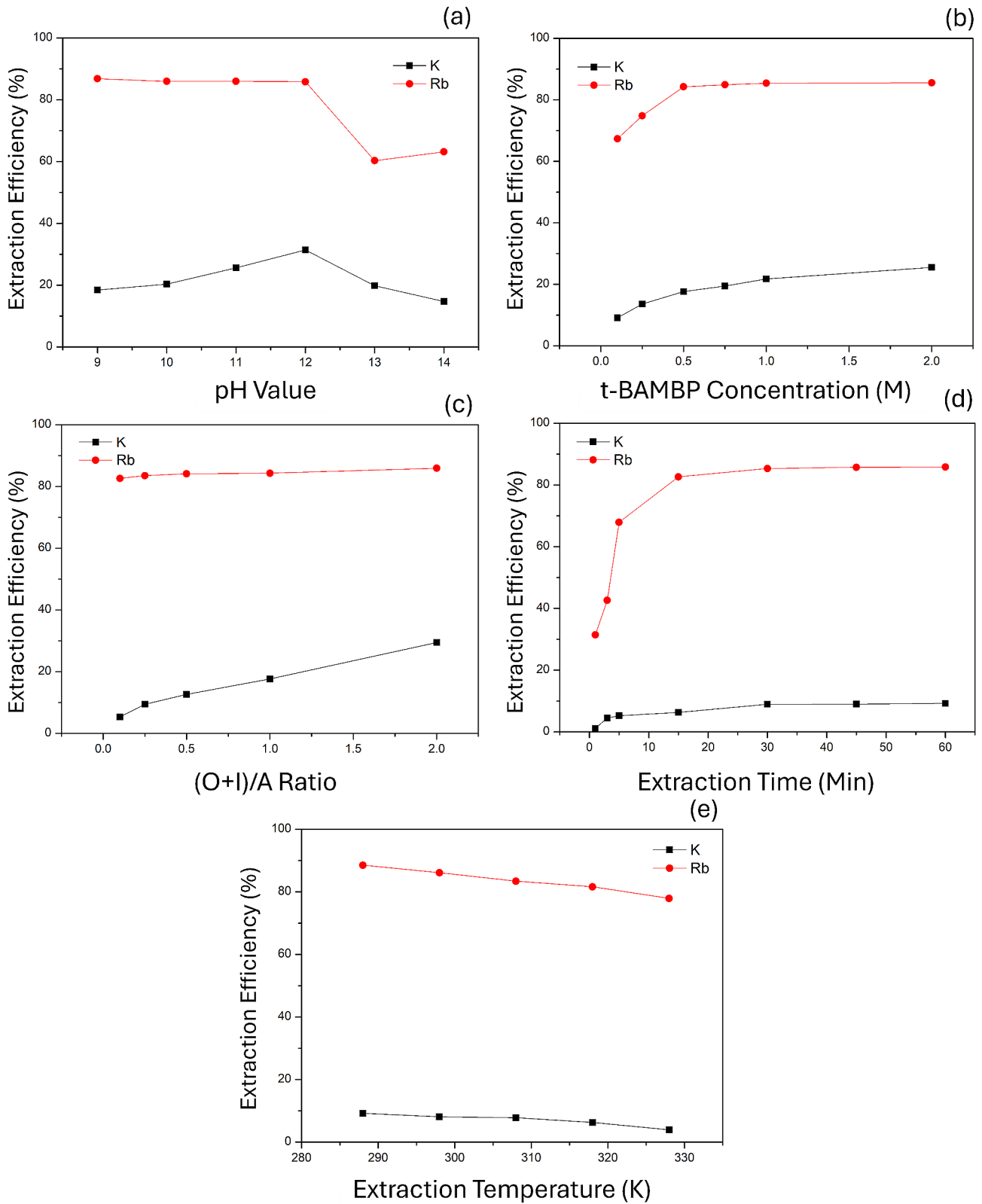


Fig. 7 Extraction efficiencies of K and Rb at different (a) pH values (b) t-BAMBP concentrations (c) (O+I)/A ratios (d) extraction time (e) extraction temperature

of metals at higher temperatures. In addition, the viscosity of $C_2mimNTf_2$ would be smaller when temperature increased, bringing about the solvents and brine mix more completely (The viscosities of $C_2mimNTf_2$ at different temperatures are in Table S6). To summarize, the optimal operating temperature chosen in this part was 298 K to reduce energy consumption and acquire more rubidium resources.

After optimizing the extraction temperature, Fig. 8 depicts the relationship between the distribution ratio in the logarithm scale and $1/T$. Through Fig. 8, Eqs. (4) and (5), the enthalpy change can be calculated, and the value is -15 kJ mol^{-1} . Negative ΔH means that the extraction reaction is exothermic, and a proper decrease in the temperature is advantageous to the reaction. Furthermore, $\log D_s$ at different temperatures are positive, so ΔG_s are negative at each temperature, representing the rubidium extraction through the $t\text{-BAMBP}/C_2mimNTf_2$ system spontaneous in this research. Although the reaction of rubidium extraction through the $t\text{-BAMBP}/C_2mimNTf_2$ system was analyzed in this study, the different

characteristics between $t\text{-BAMBP}$ and $C_2mimNTf_2$ may make distinct results. For example, if the $t\text{-BAMBP}$ concentration is low, the extraction reaction may be dominated by $C_2mimNTf_2$, leading to the unlike thermodynamics data. Therefore, it should be carefully analyzed using this system under different conditions.

$$\log D_s = -\frac{\Delta H}{2.303RT}$$

(4)

$$\Delta G_s = -2.303RT \log D$$

(5)

3.2.6 Stripping process

After the ionic extraction process, the concentrations of potassium and rubidium in the $t\text{-BAMBP}/C_2mimNTf_2$ system were 559 and 413 mg L^{-1} , respectively. Different reagents, including HNO_3 , HCl , H_2SO_4 , and NH_4OH , were employed to strip rubidium to the aqueous phase. The fixed parameters were 1 M, (O+I)/A ratio 1, stripping time for 15 min, and stripping temperature at 298 K.

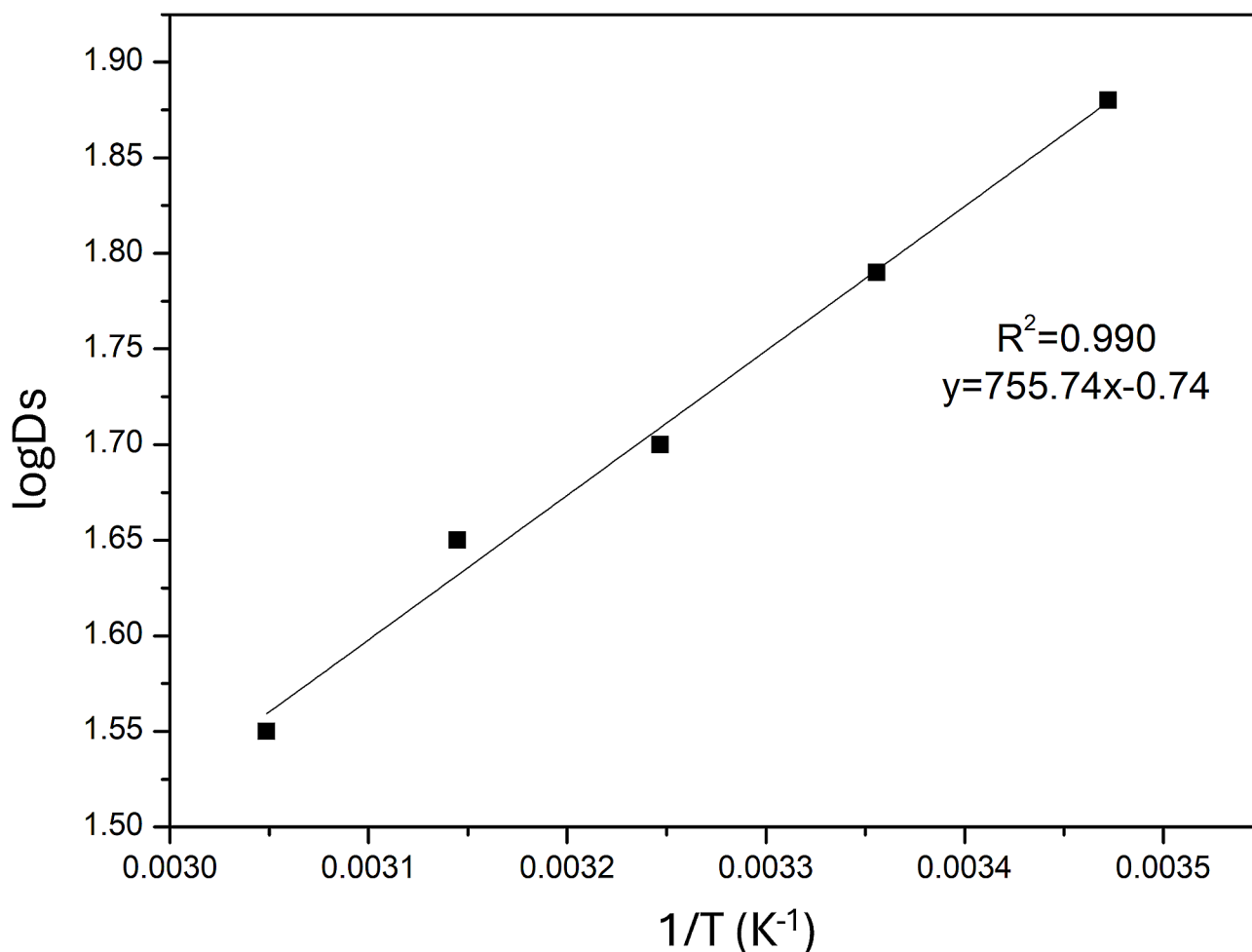


Fig. 8 Relationship of distribution ratio in logarithm scale with $1/T$

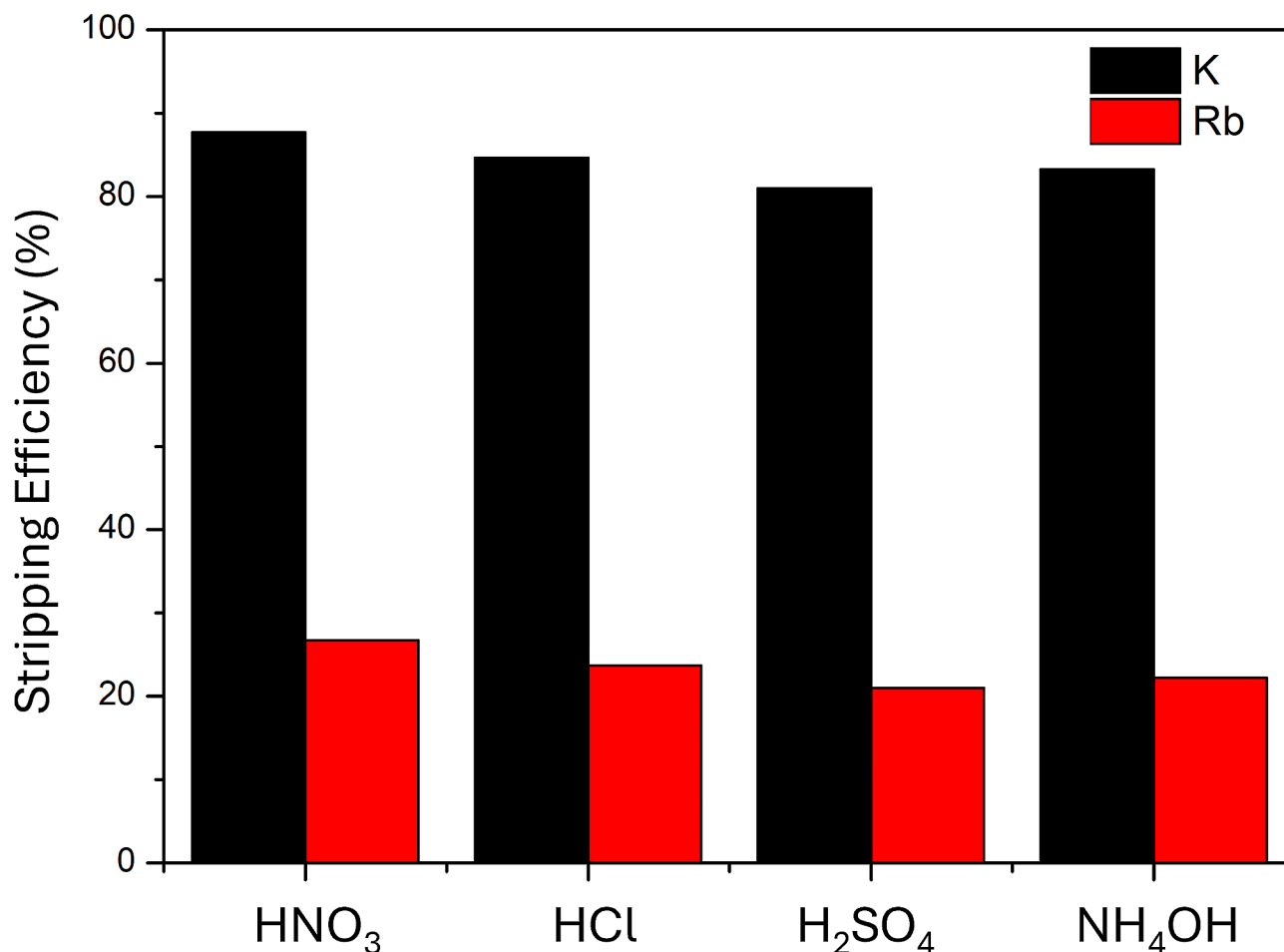


Fig. 9 Stripping efficiencies of K and Rb through different reagents

It can be discovered in Fig. 9 that both acids and alkaline solutions would strip more potassium than rubidium. This is because the affinity of t-BAMBP/C₂mimNTf₂ for rubidium is stronger than that of potassium, resulting in the preferential stripping of potassium.

The reason acid solutions could strip metals is that they provide H⁺ to exchange metals from t-BAMBP. Additionally, the extraction ability of C₂mimNTf₂ is weak under the acid condition [43]. Hence, acid solutions could also strip potassium and rubidium from C₂mimNTf₂ to the aqueous phase due to the weaker affinity of metals with C₂mimNTf₂. It is also noteworthy that NH₄OH was effective in the stripping process. Because NH₄OH would make the t-BAMBP/C₂mimNTf₂ system emulsify, preventing metals from being extracted through t-BAMBP/C₂mimNTf₂. According to these findings, HNO₃, with the highest stripping efficiency, was chosen as the suitable stripping reagent, and a two-stage stripping process will be conducted to separate potassium and rubidium.

As soon as the HNO₃ was selected, its optimal concentration, stripping (O+I)/A ratio, and stripping time were investigated. Figure 10a and c demonstrate the

parameters were 2 M, (O+I)/A ratio 1, and stripping time for 10 min. Under these conditions, the stripping efficiencies of potassium and rubidium were 100 and 29%, respectively. The remaining rubidium could then be stripped in the second stripping process under 2.5 M HNO₃, (O+I)/A ratio 1, and stripping time for 15 min. After a two-stage stripping process, the concentrations of metals are in Table 3.

3.3 Comparison of ion exchange procedure and ionic liquid extraction process

After obtaining the optimal parameters of the two systems, they are compared with each other. Table 4 demonstrates that the extraction efficiency of the t-BAMBP/C₂mimNTf₂ was much higher than the adsorption efficiency of the Dowex G26 system. Besides, rubidium concentration could be enriched about ten times in the extraction process, so the rubidium resources could be acquired more. However, the selectivity of t-BAMBP and C₂mimNTf₂ was not high; therefore, it necessitated a two-stage stripping process to separate rubidium from potassium. This phenomenon would cause about 30% of

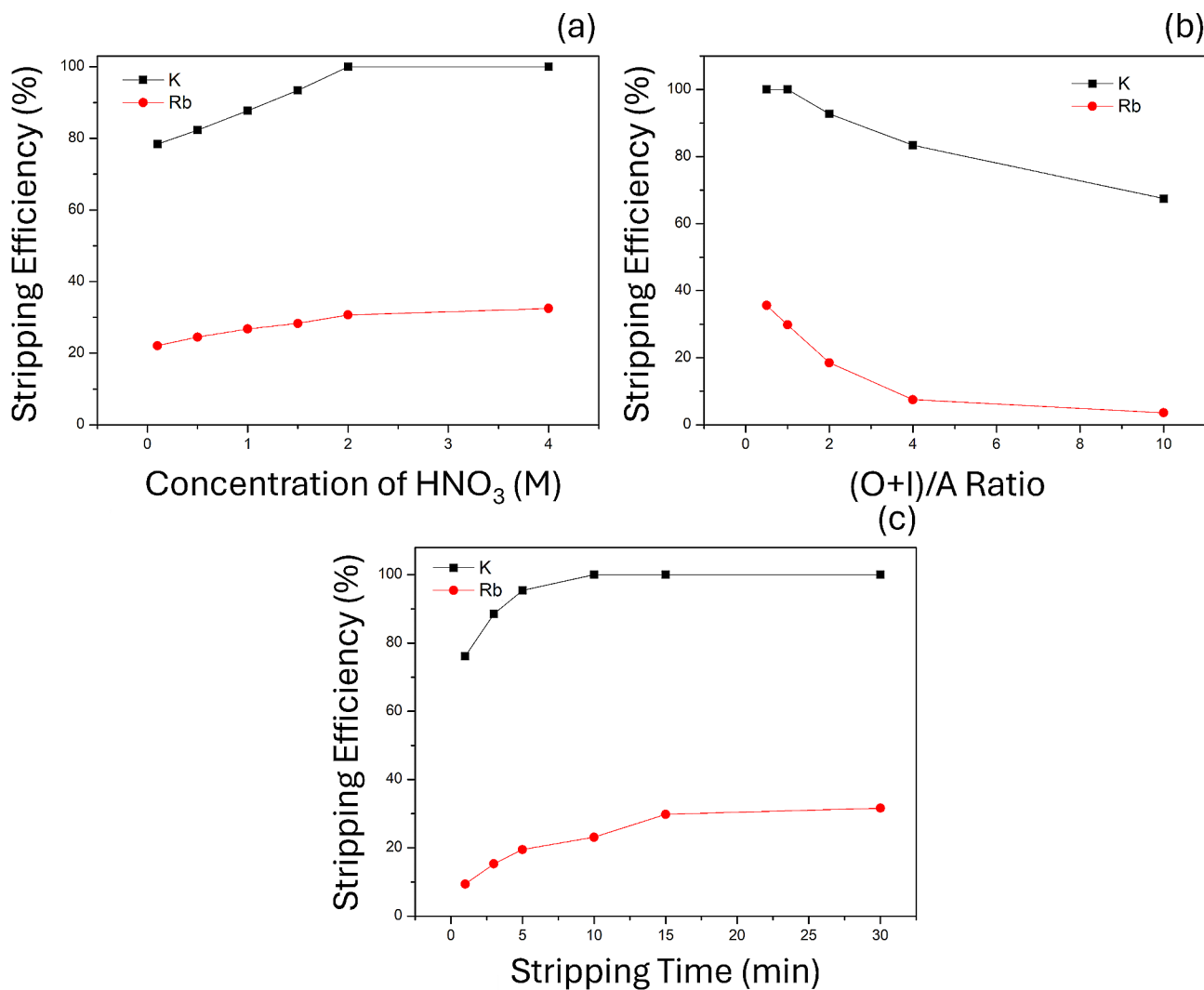


Fig. 10 Stripping efficiencies of K and Rb through HNO₃ (a) concentration of HNO₃ (b) (O+I)/A ratio (c) stripping time

Table 3 Metal concentrations after ionic liquid extraction process (Recovery efficiency of rubidium: 61%)

Elements	Rb	Na	K	Mg	Ca	Li
Concentration (mg L ⁻¹)	291.7	0.27	1.5	N.D.	N.D.	N.D.

rubidium waste and need more energy consumption. On the other hand, it may make the continuous operation of the t-BAMBP/C₂mimNTf₂ system difficult on the pilot scale or factory scale on account of the high viscosity of C₂mimNTf₂.

To sum up, the merits of the Dowex G26 system are high desorption efficiency and easy for scale operation. However, the disadvantages are low adsorption efficiency and enrichment ratio, resulting in loss of rubidium resources. The advantages of the t-BAMBP/C₂mimNTf₂ system are high extraction efficiency and enrichment ratio, but the drawbacks are the high cost of t-BAMBP and C₂mimNTf₂ and the challenges for continuous operation. Therefore, these systems still need to improve and

can be chosen under specific situations to achieve maximum benefit.

4 Conclusions

This research aimed to separate rubidium from desalination brine using the Dowex G26 and t-BAMBP/C₂mimNTf₂ systems. The results reveal that the optimal adsorption parameters were pH 9, L/S ratio of 1000, adsorption period for 4 min, and at 308 K, and the desorption conditions were 2 M of HCl, L/S ratio 200, and desorption period for 64 min. Under these situations, the adsorption capacity and desorption efficiency were 14 mg g⁻¹ and 93%. In addition, the optimal extraction parameters of the t-BAMBP/C₂mimNTf₂ system were

Table 4 Comparison of the Dowex G26 and t-BAMBP/ C_2 mimNTf₂ systems

System	Parameters	Efficiencies, %
Dowex G26	Adsorption procedure pH 9, L/S ratio of 1000, adsorption period for 4 min, and 308 K Desorption procedure 2 M HCl, L/S ratio 200, and desorption period for 64 min	30 93
t-BAMBP/ C_2 mimNTf ₂	Extraction process pH 9, 0.5 M t-BAMBP, (O + I)/A ratio of 0.1, extraction time for 30 min, and 298 K Stripping process 2 M HNO ₃ , (O + I)/A ratio 1, and stripping time for 10 min 2.5 M HNO ₃ , (O + I)/A ratio 1, and stripping time for 15 min	86 71

pH 9, 0.5 M t-BAMBP, (O+I)/A ratio of 0.1, extraction time for 30 min, and at 298 K, and rubidium resources required a two-stage stripping process to be circulated. Under these conditions, the extraction and stripping efficiencies were 86 and 71%, respectively. In a nutshell, although both systems have different merits and drawbacks, they are prospective methods to achieve the goal of resources circulation, wastewater treatment, and environmental protection. If more resources and methods can be recovered from brine and conducted; brine waste from disposal to utilization will be prevalent in the future.

Supplementary Information

The online version contains supplementary material available at <https://doi.org/10.1186/s42834-024-00212-2>.

Supplementary Material 1

Acknowledgements

This research was supported by the Laboratory of Resource Circulation in the Department of Resources Engineering, National Cheng-Kung University. Moreover, this work was financially supported by the Hierarchical Green-Energy Materials (Hi-GEM) Research Center, from The Featured Areas Research Center Program within the framework of the Higher Education Sprout Project by the Ministry of Education (MOE) in Taiwan.

Authors' contributions

Conceptualization, C. H. L.; methodology, C. H. L. and W. S. C.; validation, C. H. L. and F. W. L.; formal analysis, C. H. L.; investigation, C. H. L.; data curation, W. S. C.; writing—original draft preparation, C. H. L.; writing—review and editing, C. H. L. and F. W. L.; visualization, C. H. L.; supervision, W. S. C. All authors have read and agreed to the published version of the manuscript.

Funding

This research received no external funding.

Data availability

Not applicable.

Declarations

Competing interests

The authors declare they have no competing interests.

Received: 31 May 2023 / Accepted: 11 April 2024

Published online: 10 May 2024

References

- Djuma H, Bruggeman A, Eliades M, Lange MA. Non-conventional water resources research in semi-arid countries of the Middle East. *Desalin Water Treat.* 2016;57:2290–303.
- UNESCO. The United Nations World Water Development Report 4: Managing Water under Uncertainty and Risk. Paris: United Nations Educational, Scientific and Cultural Organization; 2012.
- Mavukkandy MO, Chabib CM, Mustafa I, Al Ghaferi A, AlMarzooqi F. Brine management in desalination industry: From waste to resources generation. *Desalination.* 2019;472:114187.
- Panagopoulos A, Haralambous KJ, Loizidou M. Desalination brine disposal methods and treatment technologies - A review. *Sci Total Environ.* 2019;693:133545.
- Krishna HJ. Introduction to desalination technologies. In: Arroyo JA editor. *The Future of Desalination in Texas (Volume 2): Technical Papers, Case Studies, and Desalination Technology Resources.* Austin: Texas Water Development Board; 2004.
- Nair M, Kumar D. Water desalination and challenges: The Middle East perspective: a review. *Desalin Water Treat.* 2013;51:2030–40.
- Semiat R. Energy issues in desalination processes. *Environ Sci Technol.* 2008;42:8193–201.
- Ghalavand Y, Hatampour MS, Rahimi A. A review on energy consumption of desalination processes. *Desalin Water Treat.* 2015;54:1526–41.
- Jones E, Qadir M, van Vliet MTH, Smakhtin V, Kang SM. The state of desalination and brine production: A global outlook. *Sci Total Environ.* 2019;657:1343–56.
- Sharkh BA, Al-Amoudi AA, Farooque M, Fellows CM, Ihm S, Lee S, et al. Seawater desalination concentrate—a new frontier for sustainable mining of valuable minerals. *Npj Clean Water.* 2022;5:9.
- Panagopoulos A, Haralambous KJ. Minimal Liquid Discharge (MLD) and Zero Liquid Discharge (ZLD) strategies for wastewater management and resource recovery— Analysis, challenges and prospects. *J Environ Chem Eng.* 2020;8:104418.
- Panagopoulos A. A comparative study on minimum and actual energy consumption for the treatment of desalination brine. *Energy.* 2020;212:118733.
- Ziolkowska JR, Reyes R. Prospects for desalination in the United States— Experiences from California, Florida, and Texas. In: Ziolkowska JR, Peterson JM, editors. *Competition for Water Resources.* Amsterdam: Elsevier; 2017. p. 298–316.
- Gude GG. *Emerging Technologies for Sustainable Desalination Handbook.* Amsterdam: Elsevier; 2018.
- Heck N, Petersen KL, Potts DC, Haddad B, Paytan A. Predictors of coastal stakeholders' knowledge about seawater desalination impacts on marine ecosystems. *Sci Total Environ.* 2018;639:785–92.
- Backer SN, Bouaziz I, Kallayi N, Thomas RT, Preethikumar G, Takriff MS, et al. Review: Brine solution - Current status, future management, and technology development. *Sustainability.* 2022;14:6752.
- Bello AS, Zouari N, Da'ana DA, Hahladakis JN, Al-Ghouthi MA. An overview of brine management: Emerging desalination technologies, life cycle assessment, and metal recovery methodologies. *J Environ Manage.* 2021;288:112358.
- Zhang X, Zhao W, Zhang Y, Jegatheesan V. A review of resource recovery from seawater desalination brine. *Rev Environ Sci Bio.* 2021;20:333–61.
- Dindi A, Quang DV, Abu-Zahra MRM. Simultaneous carbon dioxide capture and utilization using thermal desalination reject brine. *Appl Energy.* 2015;154:298–308.
- El-Naas MH, Mohammad AF, Suleiman MI, Al Musharfy M, Al-Marzouqi AH. A new process for the capture of CO₂ and reduction of water salinity. *Desalination.* 2017;411:69–75.
- Yoo Y, Kang D, Park S, Park J. Carbon utilization based on post-treatment of desalinated reject brine and effect of structural properties of amines for CaCO₃ polymorphs control. *Desalination.* 2020;479:114325.

22. Kang D, Yoo Y, Park J. Accelerated chemical conversion of metal cations dissolved in seawater-based reject brine solution for desalination and CO₂ utilization. *Desalination*. 2020;473:114147.
23. Mustafa J, Mourad AAHI, Al-Marzouqi AH, El-Naas MH. Simultaneous treatment of reject brine and capture of carbon dioxide: A comprehensive review. *Desalination*. 2020;483:114386.
24. Lee CH, Chen PH, Chen WS. Recovery of alkaline earth metals from desalination brine for carbon capture and sodium removal. *Water*. 2021;13:3463.
25. Habashi F. Recent trends in extractive metallurgy. *J Min Metall B*. 2009;45:1–13.
26. Free ML. *Hydrometallurgy: Fundamentals and Applications*. Berlin: Springer; 2021.
27. Helfferich FG. *Ion Exchange*. New York: Dover; 1995.
28. Nachod FC, Schubert J. *Ion Exchange Technology*. Amsterdam: Elsevier; 2013.
29. Lei Z, Chen B, Koo YM, MacFarlane DR. Introduction: ionic liquids. *Chem Rev*. 2017;117:6633–5.
30. Lee CH, Chen WS. Extraction of cesium from aqueous solution through t-BAMBP/C₂mimNTf₂ and recovery of cesium from waste desalination brine. *Desalin Water Treat*. 2021;235:193–9.
31. Gamez S, Garcees K, de la Torre E, Guevara A. Precious metals recovery from waste printed circuit boards using thiosulfate leaching and ion exchange resin. *Hydrometallurgy*. 2019;186:1–11.
32. Haas CN, Tare V. Application of ion exchangers to recovery of metals from semiconductor wastes. *React Polym, Ion Exc, Sorb*. 1984;2:61–70.
33. Zhu P, Chen Y, Wang LY, Zhou M. Treatment of waste printed circuit board by green solvent using ionic liquid. *Waste Manage*. 2012;32:1914–8.
34. Schaeffer N, Passos H, Billard I, Papaiconomou N, Coutinho JAP. Recovery of metals from waste electrical and electronic equipment (WEEE) using unconventional solvents based on ionic liquids. *Crit Rev Env Sci Tec*. 2018;48:859–922.
35. AliAkbari R, Marfavi Y, Kowsari E, Ramakrishna S. Recent studies on ionic liquids in metal recovery from e-waste and secondary sources by liquid-liquid extraction and electrodeposition: a review. *Mater Circ Econ*. 2020;2:10.
36. Rzelewska M, Baczynska M, Wisniewski M, Regel-Rosocka M. Phosphonium ionic liquids as extractants for recovery of ruthenium(III) from acidic aqueous solutions. *Chem Pap*. 2017;71:1065–72.
37. Mahandra H, Faraji F, Ghahreman A. Novel extraction process for gold recovery from thiosulfate solution using phosphonium ionic liquids. *ACS Sustain Chem Eng*. 2021;9:8179–85.
38. Padhan E, Sarangi K. Recovery of Nd and Pr from NdFeB magnet leachates with bi-functional ionic liquids based on Aliquat 336 and Cyanex 272. *Hydrometallurgy*. 2017;167:134–40.
39. Prusty S, Pradhan S, Mishra S. Ionic liquid as an emerging alternative for the separation and recovery of Nd, Sm and Eu using solvent extraction technique-A review. *Sustain Chem Pharm*. 2021;21:100434.
40. Chen WS, Lee CH, Ho HJ. Purification of lithium carbonate from sulphate solutions through hydrogenation using the Dowex G26 resin. *Appl Sci*. 2018;8:2252.
41. Chen WS, Chen YA, Lee CH, Chen YJ. Recycling vanadium and proton-exchange membranes from waste vanadium flow batteries through ion exchange and recast methods. *Materials*. 2022;15:3749.
42. Kostrzewa M, Staszak K, Ginter-Kramarczyk D, Kruszelnicka I, Gora W, Baraniak M, et al. Chromium(III) removal from nickel(II)-containing waste solutions as a pretreatment step in a hydrometallurgical process. *Materials*. 2022;15:6217.
43. Luo Y, Chen Q, Shen X. Complexation and extraction investigation of rubidium ion by calixcrown-C₂mimNTf₂ system. *Sep Purif Technol*. 2019;227:115704.
44. Wu H, Kudo T, Kim SY, Miwa M, Matsuyama S. Recovery of cesium ions from seawater using a porous silica-based ionic liquid impregnated adsorbent. *Nucl Eng Technol*. 2022;54:1597–605.
45. Huang D, Ma G, Lv P, Zhou Q. Extraction of rubidium ion from brine solutions by dicyclohexano-18-crown-6 / ionic liquid system. *Pol J Chem Technol*. 2023;25:61–8.
46. Li Z, Pranolo Y, Zhu Z, Cheng CY. Solvent extraction of cesium and rubidium from brine solutions using 4-tert-butyl-2-(*o*-methylbenzyl)-phenol. *Hydrometallurgy*. 2017;171:1–7.
47. Freundlich H. About adsorption in solutions. *Int J Res Phys Chem Chem Phys*. 1907;57:385–470 [In German]. <https://doi.org/10.1515/zpch-1907-5723> (Accessed 8 Apr 2024).
48. Langmuir I. The constitution and fundamental properties of solids and liquids. *Journal of the Franklin Institute*. 1917;183:102–5.
49. Lee CH, Chen WS, Wu JY. Adsorption of cesium from waste desalination brine through Dowex G26 resin and comparison with t-BAMBP/kerosene and t-BAMBP/C₂mimNTf₂ systems. *Desalin Water Treat*. 2021;236:69–75.
50. Chen WS, Lee CH, Chung YF, Tien KW, Chen YJ, Chen YA. Recovery of rubidium and cesium resources from brine of desalination through t-BAMBP extraction. *Metals*. 2020;10:607.
51. Li Z, Pranolo Y, Zhu Z, Cheng CY. Solvent extraction of cesium and rubidium from brine solutions using 4-tert-butyl-2-(*o*-methylbenzyl)-phenol. *Hydrometallurgy*. 2017;171:1–7.

Publisher's Note

Springer Nature remains neutral with regard to jurisdictional claims in published maps and institutional affiliations.